

Rice Classification Using Spatio-Spectral Deep Convolutional Neural Network

Itthi Chatnuntawe^a, Kittipong Tantisansom^a, Paisan Khanchaitit^a, Thitikorn Boonkoom^a,
Berkin Bilgic^{b,c}, Ekapol Chuangsuwanich^d

^aNational Nanotechnology Center, National Science and Technology Development Agency,
Pathum Thani, Thailand

^bAthinoula A. Martinos Center for Biomedical Imaging, Charlestown, MA, USA

^cHarvard Medical School, Boston, MA, USA

^dComputer Engineering Department, Chulalongkorn University, Bangkok, Thailand

Abstract

Rice has been one of the staple foods that contribute significantly to human food supplies. Numerous rice varieties have been cultivated, imported, and exported worldwide. Different rice varieties could be mixed during rice production and trading. Rice impurities could damage the trust between rice importers and exporters, calling for the need to develop a rice variety inspection system. In this work, we develop a non-destructive rice variety classification system that benefits from the synergy between hyperspectral imaging and deep convolutional neural network (CNN). The proposed method uses a hyperspectral imaging system to simultaneously acquire complementary spatial and spectral information of rice seeds. The rice varieties are then determined from the acquired spatio-spectral data using a deep CNN. As opposed to several existing rice variety classification methods that require hand-engineered features, the proposed method automatically extracts features from the raw sensor data. As demonstrated using two types of rice datasets, the proposed method achieved up to 8% relative improvement in the classification accuracy compared to the commonly used classification methods based on support vector machines.

1. Introduction

Rice has been one of the most widely consumed foods for a large part of human population. Numerous different rice varieties are imported and exported worldwide, making it the backbone of many countries' economy. Rice seeds of different varieties can be accidentally or intentionally mixed during any of the steps in a rice production pipeline, introducing impurities. These impurities could damage the trust between rice importers and exporters, calling for the need to develop a reliable rice variety inspection system.

Several methods based on biological or chemical techniques such as genetic markers have been proposed to determine rice varieties [1–3]. Although these methods are very accurate, they are destructive techniques that are costly and time-consuming, making them unsuitable for mass inspection. Being limited to batch sampling, these techniques cannot truly assess the purity of the rice seeds under inspection. To circumvent these limitations, non-destructive rice inspection systems that use a combination of optical imaging and multi-variate data analysis

techniques have been proposed [4–15]. For these techniques, the data from rice seeds are acquired using an optical imaging system. Some information that characterizes the acquired data (commonly called features) is then extracted as input for a data classification algorithm.

There are two types of features that are frequently extracted for these methods: spatial and spectral features. Common spatial features that describe the visual appearance of a rice seed include shape, morphological, and textural features. Several research groups have demonstrated promising classification accuracies of the rice varieties that are visually distinguishable, using only spatial features acquired with a digital camera [4–9] and with some additional equipment such as a microscope [10].

While a typical digital camera provides only partial information in the visible range, other types of equipment such as a hyperspectral imaging camera can be used to acquire information from a wider range of the electromagnetic spectrum. A typical hyperspectral imaging camera can provide both spatial and spectral information in a specific portion of the electromagnetic spectrum. For example, a spectrum that contains the information on chemical properties at each spatial location can be acquired using a near-infrared hyperspectral imaging camera. It has been demonstrated that rice panicles classification [11] and rice variety classification [12] can be performed successfully by using only the spectral information acquired with a hyperspectral imaging system. Recently, rice classification systems that use both spatial and spectral features have been proposed [13–15]. These systems use a hyperspectral imaging camera to acquire data with both spatial and spectral information. They have demonstrated that using both spatial and spectral features resulted in higher classification accuracies, compared to the case when only spatial or spectral features were used.

Although the existing works have shown promising results, they rely on hand-engineered features that require extensive domain specific knowledge. Inspired by the desire to bypass a predefined feature extraction step, deep learning, a subfield of machine learning that stems from artificial neural networks, has emerged as an alternative to conventional classification methods. Having an ability to represent data with multiple levels of abstractions, deep learning has been demonstrated to be comparable to, or surpass existing methods, achieving state-of-the-art performances in a wide range of applications such as image recognition [16–20], speech recognition [21–24], medical imaging processing and analysis [25–27], hyperspectral imaging [28,29], and bioinformatics [30,31].

The purpose of this work was to develop a non-destructive technique to improve the reliability of rice variety classification. The proposed technique uses a hyperspectral imaging system to simultaneously acquire spatial and spectral information of rice seeds. The rice varieties are then determined from the acquired spatio-spectral data using a classification method that is developed based on deep convolutional neural network (CNN). As opposed to existing rice variety classification methods that require hand-engineered feature extractions, the proposed method automatically extracts features from the data. Furthermore, while the existing methods involve multiple subsequent data processing steps and hence suffer from error propagation between the subsequent steps, the proposed classification method is a single-step method that does not encounter such a problem.

2. Material and Methods

Typical rice variety classification systems consist of two parts: data acquisition, and data processing and classification. In this work, as shown in Figure 1, we used a near-infrared hyperspectral imaging system to acquire data because it is a rapid data acquisition method that

provides both spatial and spectral information without damaging the samples under inspection. The acquired spatio-spectral data, which are commonly called datacubes, had three dimensions: two spatial dimensions and one spectral dimension. While the spatial dimensions provided information on the visual appearances of the rice seeds, the spectral dimension provided complementary information on their chemical properties. From the acquired datacubes, the rice varieties were then determined using data processing and classification methods.

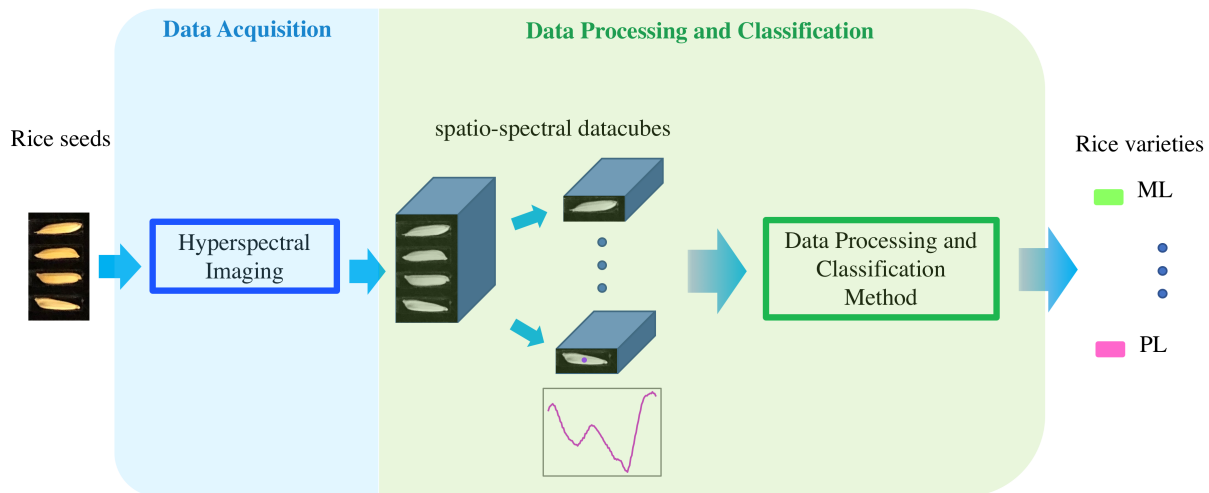


Figure 1. Example of a rice variety classification system based on hyperspectral imaging.

2.1 Data acquisition

2.1.1 Hyperspectral imaging system

A line-scan hyperspectral imaging system was constructed as depicted in Figure 2 in a dark room. The system consisted of the following components: (1) a near-infrared hyperspectral imaging camera that covers the 900 - 1700 nm spectral range with a spectral resolution of 5.49 nm (Pika NIR, Resonon Inc., USA), (2) four 50-watt halogen lamps to illuminate the region of interest (GU5.3, Philips), (3) a conveyor belt (Oriental Motor Co., Ltd., Japan), (4) a 90W, US-52 speed controller for the conveyor belt (AP Electric, Thailand), and (5) a computer to collect and process the acquired data.

2.1.2 Datacube acquisition

Prior to data acquisition, the halogen lamps were preheated for 30 minutes to allow them to reach a stable operating condition. The datacubes of rice seeds were acquired using the line-scan hyperspectral imaging camera. Only one spatial dimension (one line) and spectral dimension of the rice seeds that were located right under the hyperspectral imaging camera were acquired at a time. In order to collect the data from the second spatial dimension, the conveyor belt was used to move the rice seeds to different locations over time. The speed controller was used to control the conveyor belt's speed to maintain a realistic aspect ratio of the acquired data. The data from the hyperspectral camera were then sent to the computer for further data processing. The datacubes of all the rice seeds were acquired in the same geometric orientation as shown in Figure 2.

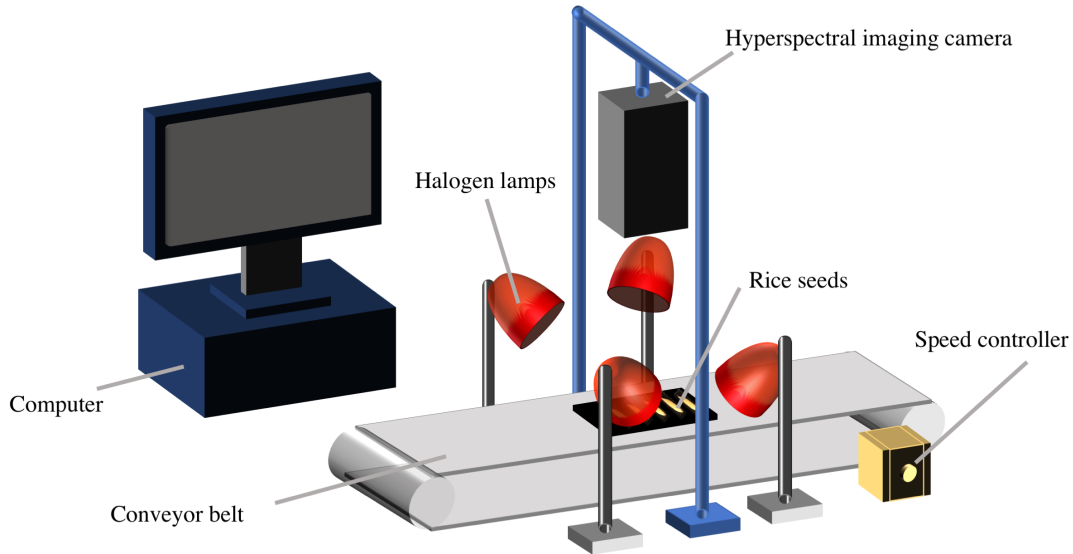


Figure 2. The line-scan hyperspectral imaging system used for data acquisition.

2.2 Data processing and classification

2.2.1 Support vector machine (SVM)

SVM is a supervised learning method that is widely used for regression and classification frameworks due to its ability to effectively handle high dimensional data, even when the number of samples is lower than the number of input dimensions [32,33]. Some information that characterizes the raw data (i.e., features) is typically extracted and used as input for the SVM. If used for classification tasks, SVM constructs a hyperplane or a set of hyperplanes that represents the largest separation of data from different classes in the feature space and uses the constructed hyperplanes to classify unseen test data. The accuracy of SVM highly depends on the quality of features extracted from the data. For rice classification, two types of features are typically extracted from each rice seed (Figure 3): spatial features [4–10,13–15] and spectral features [11–15]. Then, the features are typically standardized and used as SVM inputs to determine the variety of each rice seed.

2.2.1.1 Spatial feature extraction

Similar to the spatial features used in recent works [4–10,13–15], six textural and eleven morphological features were used in this work. For each rice seed, a sum-of-squares (SS) image was computed by summing the squared-magnitudes of the datacube along the spectral dimension.

The textural features were extracted directly from the resulting SS image by computing the following features of a gray-level co-occurrence matrix [34] as defined in [35]: dissimilarity, homogeneity, angular second moment, energy, and correlation.

For morphological features, three data processing methods were sequentially performed on the SS image to get a clean binary image (also called a mask) that will be used for morphological feature extractions. First, the SS image was filtered using a Gaussian kernel to mitigate unwanted artifacts. Then, adaptive thresholding was performed to get an initial mask (1

for the pixels that belong to the rice seed, and 0 otherwise). Finally, morphological opening and closing operations were performed to clean up the mask.

With the resulting mask, eleven morphological features were extracted: surface area, perimeter, perimeter-to-area ratio, major axis length, minor axis length, first eccentricity, standard deviation of the radii, minimum radius, maximum radius, maximum-to-minimum radius ratio, and Haralick ratio. While the surface area, perimeter, and perimeter-to-area ratio were calculated directly from the mask, an additional processing step was required to extract the other morphological features. Specifically, an ellipse was fit to the mask to approximately represent the rice seed boundary. The ellipse with the lowest fitting error in a least-squares sense was kept. The radii were defined as the distances from the centroid of the ellipse to the contour points. The Haralick ratio was defined as the ratio of the mean radius to the standard deviation of the radii.

2.2.1.2 Spectral feature extraction

While spatial features provide information on the visual appearances, spectral features provide complementary information on chemical properties of the rice seeds. The mean spectrum of each datacube over a region of interest (ROI) was used as spectral features. In this work, an ROI was chosen to be the region that contained all voxels within the rice seed.

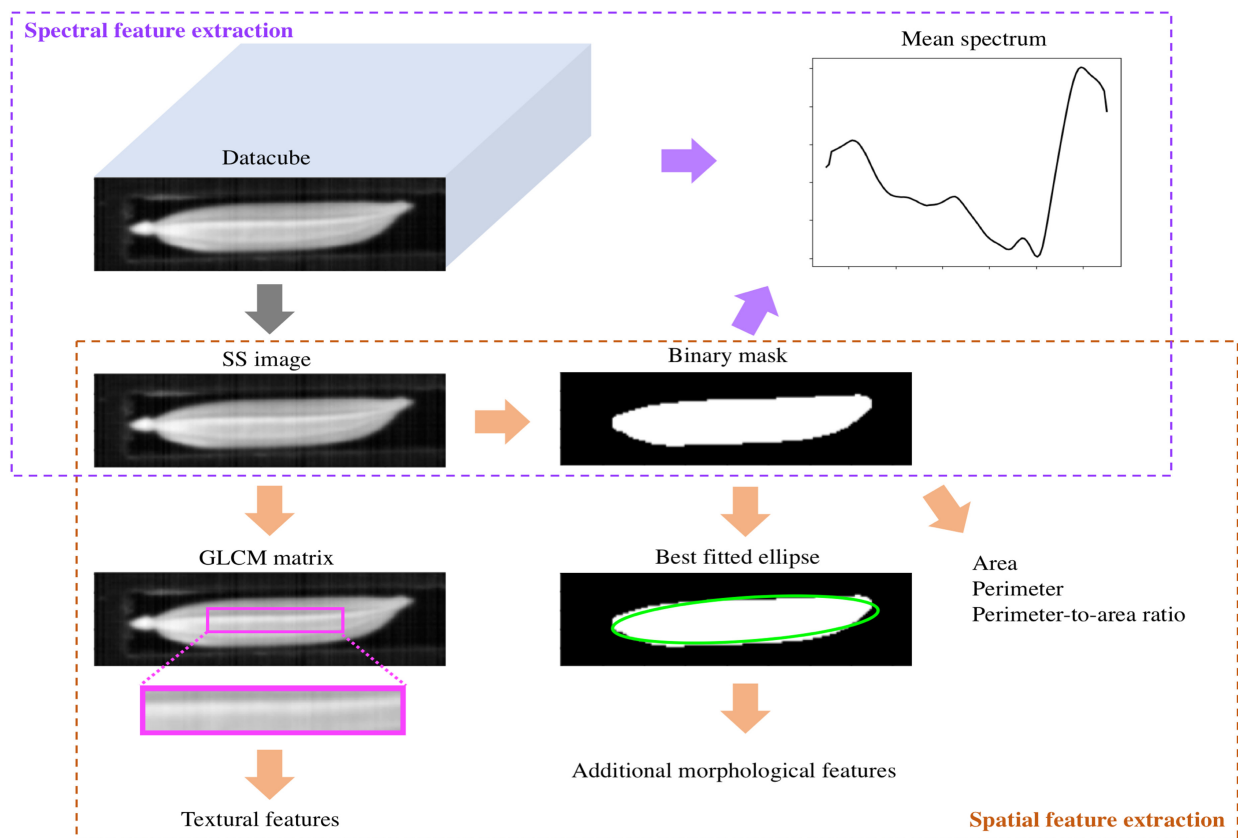


Figure 3. The spatial and spectral feature extraction processes for the SVM-based rice classification methods in this work. Multiple sequential data processing steps are performed to extract the features.

2.2.2 Proposed: deep convolutional neural network

Deep CNN is a class of machine learning technique that was invented with an inspiration from visual neurosciences [36]. A deep CNN consists of a series of processing layers. As the data enter the network, they go through a cascade of linear and nonlinear mathematical operations of each processing layer. The processed data from one layer are used as inputs for the next layer. Each layer transforms the representation of its inputs into another representation that is more complex and abstract. Consequently, a deep CNN learns how to represent data with multiple levels of abstractions by itself, as opposed to conventional classification methods, which rely on predefined feature extractions that have been developed from human past experiences. Please refer to Refs. [37,38], for example, for fundamentals of and recent advances in deep learning.

In this work, we developed a data classification method based on deep CNN with hundreds of processing layers. We modified and extended dense convolutional network (DenseNet) [20] to improve spatio-spectral data classification. The proposed method takes advantages of dense connections [20], batch normalization [39], and dropout [40] to aid the training process of such a deep network. Dense connections help improve the information flow throughout the network, which results in easier training processes of neural networks, especially for the deep ones. Batch normalization helps mitigate the covariance shift problem [41], which allows us to use high values of the learning rate, accelerating the training process. Dropout is introduced to prevent the network from overfitting the data, and hence potentially increases the classification accuracy of unseen samples.

As described in Sections 2.2.1.1 and 2.2.1.2, existing rice variety classification methods involve a separate feature extraction process that consists of multiple sequential data processing steps. Each of the sequential steps is usually associated with some adjustable parameters (e.g., a threshold value of the adaptive thresholding operation), and requires good parameter tuning to obtain acceptable performance. If suboptimal parameters are chosen for one of the steps, it could adversely affect the performances of all the subsequent steps, including the classification step. For instance, if a far-from-optimal value is used for the adaptive thresholding step, we could get a binary mask that does not represent the rice seed well. Consequently, both spatial and spectral feature extraction processes, which heavily rely on the mask, will be inaccurate, leading to decreased classification accuracy. To prevent such error propagation, we used a deep CNN to simultaneously perform feature extractions and rice variety classification. The entire datacube is used as features, removing the need for multi-step feature extractions.

Another key advantage of the proposed method is that it can automatically discover the features needed for classification. Without relying on hand-engineered features that require extensive domain specific knowledge and good feature engineering skill, the proposed method can potentially discover data presentations that truly matter for classification automatically. Moreover, while recent rice classification methods treat spatial feature extraction and spectral feature extraction as two separate processes, and create “spatio-spectral” features by simply concatenating the extracted spatial and spectral features [13–15], the proposed method could create genuine spatio-spectral features because it performs feature extraction directly on the datacube, which provides direct access to both spatial and spectral information.

2.3 Experiments

Using two types of rice datasets, we compared the performance of the proposed method to three different variants of the method commonly used for rice classification: SVM with spatial features, SVM with spectral features, and SVM with both spatial and spectral features.

2.3.1 Datasets

Two rice datasets, consisting of processed rice and paddy rice datasets, were acquired from the hyperspectral imaging system as described in Section 2.1 and then used to assess the performances of the classification methods. The processed rice dataset served as a proof-of-concept since the varieties were easily distinguishable by the visual appearances and/or spectral profiles of the rice seeds. The paddy rice dataset represented a real-world scenario in Thailand, where the rice varieties in this dataset have been frequently mistaken for the others because they have very similar visual appearances and spectral profiles, posing a serious challenge to rice inspection systems. In this case, without a reliable inspection system, relatively low quality rice varieties could be mistaken for high quality rice varieties and sold at higher-than-normal prices, damaging the trust in rice import and export industries. Figure 4 shows examples of rice seeds from each rice variety in the datasets along with the mean spectra.

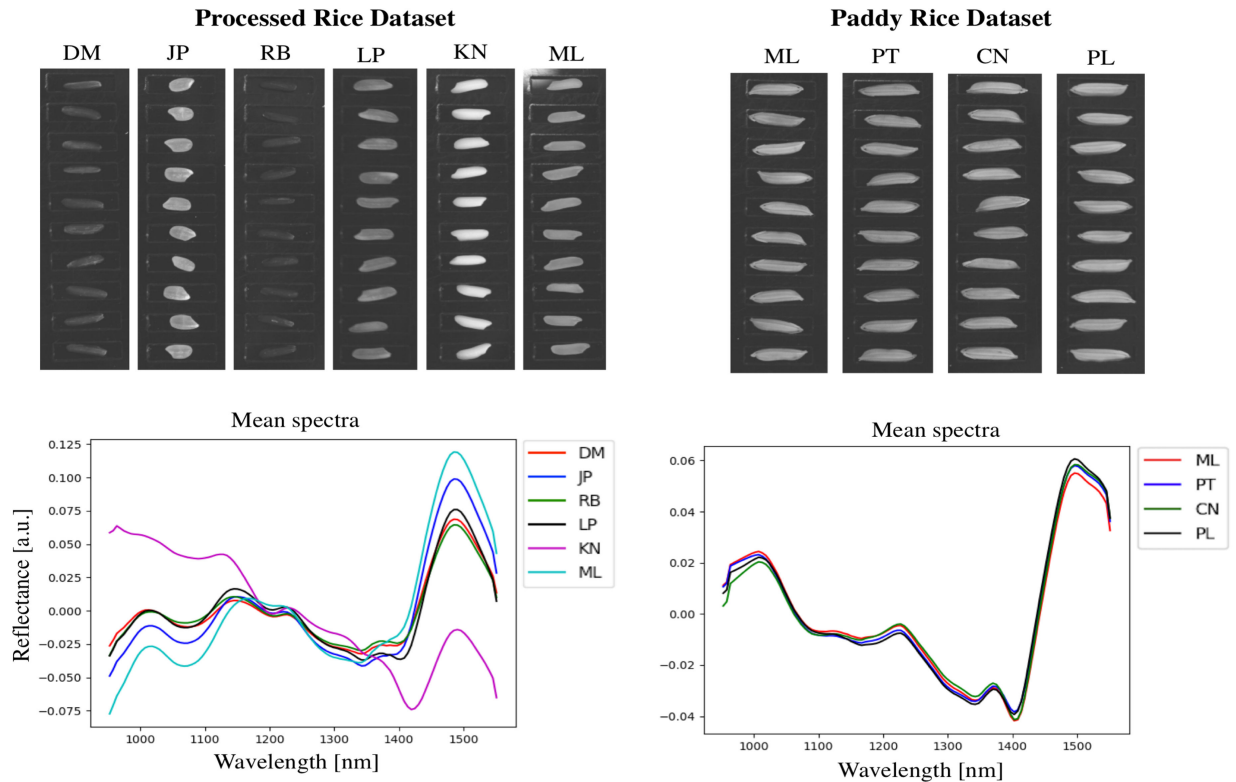


Figure 4. Examples of the rice seeds from each rice variety in the processed (left) and paddy (right) datasets along with the mean reflectance spectra (after being demeaned and filtered).

2.3.1.1 Processed rice

In this work, processed rice referred to both brown rice (paddy rice with outer hull removed) and white rice (paddy rice with outer hull and almost all bran and germ removed). Six varieties of processed rice were obtained from a seed production company in Thailand: Daeng Mun Pooh (DM), Uruchimai Japonica (JP), Riceberry (RB), Leuang Patew (LP), Kiaw Ngu (KN), and Khao Dawk Mali 105 (i.e., Thai jasmine rice, ML). Using the hyperspectral imaging system, 232 datacubes were acquired for each rice variety (one datacube per rice seed), resulting in a total 1,392 datacubes. Each acquired datacube was a 50 x 170 x 110 matrix. Specifically, each datacube consisted of images of size 50 x 170 pixels with each pixel containing 110 spectral bands, ranging from 950 nm to 1550 nm.

2.3.1.2 Paddy rice

Four Thai rice varieties were obtained from the Thai Rice Department of the Ministry of Agriculture and Cooperatives: Khao Dawk Mali 105 (ML), Pathum Thani 1 (PT), Chai Nat 1 (CN), and Phitsanulok 2 (PL). Compared to the first dataset, these varieties had much more similar visual appearances and spectral profiles. Using the same hyperspectral imaging system, 414 datacubes were acquired for each rice variety, resulting in a total 1,656 datacubes. Each acquired datacube was a 50 x 170 x 110 matrix.

2.3.2 Implementation details

The acquired datacubes of the rice seeds were randomly split into training and test data: 85% for training and 15% for testing. The training data were used to optimize model parameters and train a classifier. The test data were used to assess the performance of the trained classifier. All the data processing and classification methods were implemented in Python, and run on a workstation with 64 Intel Xeon E5-2698 processors, 256 GB of memory, and an NVIDIA TITAN Xp graphics card. OpenCV [42], Scikit-learn [43], and Scikit-image [35] were mainly used for the SVM-based methods. Keras [44,45] with the Tensorflow [46] backend was used for the proposed method.

2.3.2.1 SVM-based classification methods

Three types of features were used as inputs to SVMs: spatial, spectral, and spatio-spectral features. Following existing works [13–15], a simple concatenation of the spatial and spectral features was treated as the spatio-spectral features. For all the three SVM-based classification methods, a kernel trick [32] was also used with the radial basis function kernel. The hyperparameters associated with the SVM methods were determined using cross-validation with stratified random splits on the training data with five splitting and reshuffling iterations. After the hyperparameters had been selected, the internal parameters of the classifiers (e.g., weights and biases) were optimized using all of the training data. Finally, the performances of the trained classifiers were assessed using the test dataset.

2.3.2.2 Proposed: spatio-spectral deep convolutional neural network

Prior to data classification, each datacube was normalized by its maximum value. Then, the proposed classification method based on deep CNN was used to determine the rice variety of each rice seed. The original training data (85% of the acquired datacubes) were further split into

the validation and new training data with proportions of 20% and 65% of the acquired datacubes, respectively. The validation data were used to select some of the hyperparameters: initial learning rate = 0.0005, batch size = 6, activation function = leaky ReLU, dropout rate = 0.05, and number of nodes in the classification layer = 512 and 1024 for the processed rice and paddy rice datasets, respectively. Table 1 contains the exact network configurations used in this work. The number of trainable parameters were equal to 12,198,440 and 19,296,294 for the processed rice and paddy rice datasets, respectively. After the hyperparameters had been selected, the internal parameters of the networks (e.g., weights and biases) were optimized by minimizing the cross-entropy cost function on both the new training data and validation data for 800 epochs using the Adam optimizer [47] with following parameters defined in the Keras documentation: learning rate = initial learning rate divided by the batch size, $\beta_1 = 0.9$, $\beta_2 = 0.999$, $\epsilon = 10^{-8}$, and learning rate decay = 0.01. The growth rate and compression factor as defined in Ref. [20], were set to 20 and 0.6, respectively. The training times were approximately 18 hours for both datasets.

In this work, data augmentation techniques [16,48–50] were employed to increase the amount of training data without the need to acquire more data through the data acquisition process. Specifically, more datacubes were generated by retrospectively modifying the existing datacubes with some operations consisting of shifting and flipping the datacubes. Both horizontal and vertical flippings were used. Moreover, the datacubes were randomly shifted by different amounts in the spatial domain. The maximum shifting amount was set to 4% of the number of pixels in each spatial dimension. Combining these operations, we increased the amount of training datacubes by more than 10-fold. Figure 5 shows a simplified flowchart of the proposed method.

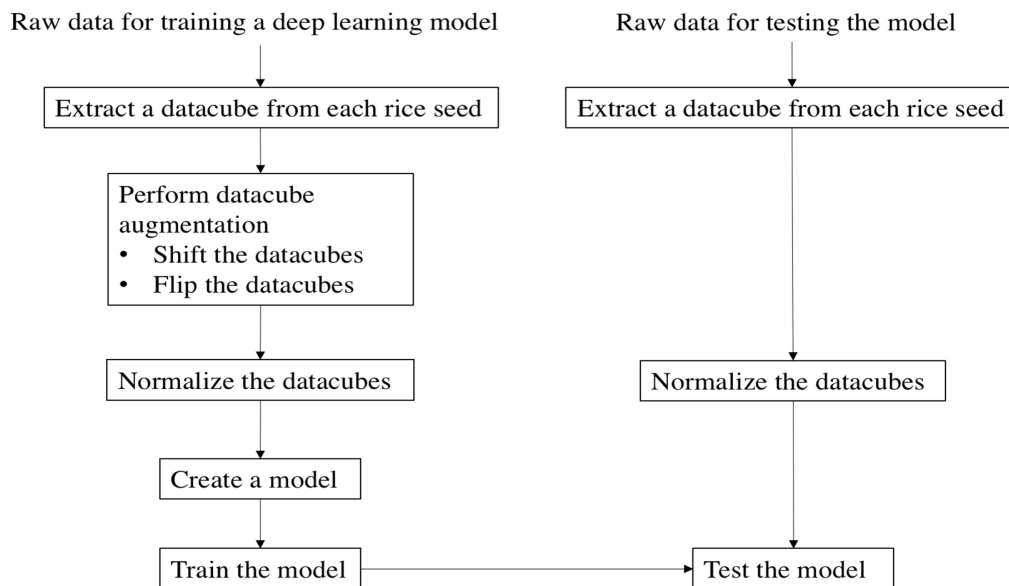


Figure 5. Simplified flowchart of the proposed method.

Layers	Output Size	Processed rice dataset	Paddy rice dataset
Conv	50 x 170 x 110	9x9 conv, stride 1	
Dense Block (1)	50 x 170 x 350	$\left[\begin{array}{l} \text{batch normalization} \\ \text{leaky ReLU} \\ 1x1 \text{ conv, stride 1} \\ 3x3 \text{ conv, stride 1} \\ \text{dropout} \end{array} \right] \times 12$	
Transition Layer (1)	25 x 85 x 210	batch normalization leaky ReLU 1x1 conv, stride 1 dropout 2x2 average pooling, stride 2	
Dense Block (2)	25 x 85 x 450	$\left[\begin{array}{l} \text{batch normalization} \\ \text{leaky ReLU} \\ 1x1 \text{ conv, stride 1} \\ 3x3 \text{ conv, stride 1} \\ \text{dropout} \end{array} \right] \times 12$	
Transition Layer (2)	12 x 42 x 270	batch normalization leaky ReLU 1x1 conv, stride 1 dropout 2x2 average pooling, stride 2	
Dense Block (3)	12 x 42 x 750	$\left[\begin{array}{l} \text{batch normalization} \\ \text{leaky ReLU} \\ 1x1 \text{ conv, stride 1} \\ 3x3 \text{ conv, stride 1} \\ \text{dropout} \end{array} \right] \times 24$	
Transition Layer (3)	6 x 21 x 450	batch normalization leaky ReLU 1x1 conv, stride 1 dropout 2x2 average pooling, stride 2	
Dense Block (4)	6 x 21 x 770	$\left[\begin{array}{l} \text{batch normalization} \\ \text{leaky ReLU} \\ 1x1 \text{ conv, stride 1} \\ 3x3 \text{ conv, stride 1} \\ \text{dropout} \end{array} \right] \times 16$	
Transition Layer (4)	3 x 10 x 462	batch normalization leaky ReLU 1x1 conv, stride 1 dropout 2x2 average pooling, stride 2	
Fully Connected Layer	512 (processed) 1024 (paddy)	512 units	1024 units
Classification Layer	6 (processed) 4 (paddy)	6 units, softmax	4 units, softmax

Table 1. Network configurations used in this work with the following details: growth rate = 20, compression factor = 0.6, dropout rate = 0.05, number of convolutional layers = 133, number of pooling layers = 4, number of batch normalizations = 68, number of leaky ReLUs = 68, and number of dropout layers = 68.

	SVM			Proposed (Spatio-spectral)
	Spatial	Spectral	Spatial and spectral	
Accuracy (Processed rice dataset)	73.8%	95.2%	94.8%	96.2%
Accuracy (Paddy rice dataset)	50.0%	77.4%	79.8%	86.3%

Table 2. Classification accuracies obtained from the four classification methods.

3. Results and Discussion

Table 2 lists the classification accuracies obtained from the four classification methods for both rice datasets. Figures 6 and 7 show the corresponding confusion matrices for the processed rice and paddy rice datasets, respectively. All of the JP rice seeds were correctly identified even when only the spatial information was used due to their distinct visual appearances. All of the KN rice seeds were perfectly identified using their unique spectral profiles. However, misclassifications were observed for the rice varieties that were more similar spatially or spectrally (such as the LP and ML varieties in the processed rice dataset, and all the varieties in the paddy rice dataset). The misclassification errors were reduced by using both spatial and spectral information. Exploiting spatio-spectral information automatically extracted from the datacubes, the proposed method based on deep CNN yielded highest rice variety classification accuracies in both cases. Since the other methods need to perform a cascade of data preprocessing steps for feature extractions, they could encounter potential error propagation between the steps, which is extremely unlikely for the proposed method, which does not require these preprocessing steps. Furthermore, the proposed method does not rely on hand-engineered features, which could be suboptimal for the given rice variety classification tasks. For instance, while the hand-engineered spatial features were successfully used to distinguish some of the rice varieties in the processed rice dataset (e.g., the JP variety versus the rest), they were not very useful for the paddy rice dataset because the spatial features of different rice varieties were very similar to each other. This observation suggests that using the predefined features might not be the most appropriate approach. Treating feature extraction as a separate process could also lead to loss of information that cannot be recovered since the datacube is typically discarded after the feature extraction process.

Having an ability to learn data representations with multiple levels of abstractions directly from the datacube by itself, the proposed method is much less susceptible to biases from human past experiences, which might be irrelevant in some cases, and hence could discover data representations that truly matter for classification. However, interpreting a trained deep CNN is complicated. Several methods based on visualizations have been proposed to help us understand a trained network better [51–55]. In this work, saliency maps were used to gain some insight into how the trained deep CNNs could have made the decision (Figure 8). An image-specific saliency map provides some information on how the decision made by a trained CNN changes with respect to a small change in each input region [51]. The regions (voxels) in the saliency map with high values contribute more towards the decision (i.e., predicted rice variety), compared to the low values regions. As shown in Figure 8, the trained deep CNNs were able to automatically

Processed Rice Dataset: Confusion Matrices and Classification Accuracies

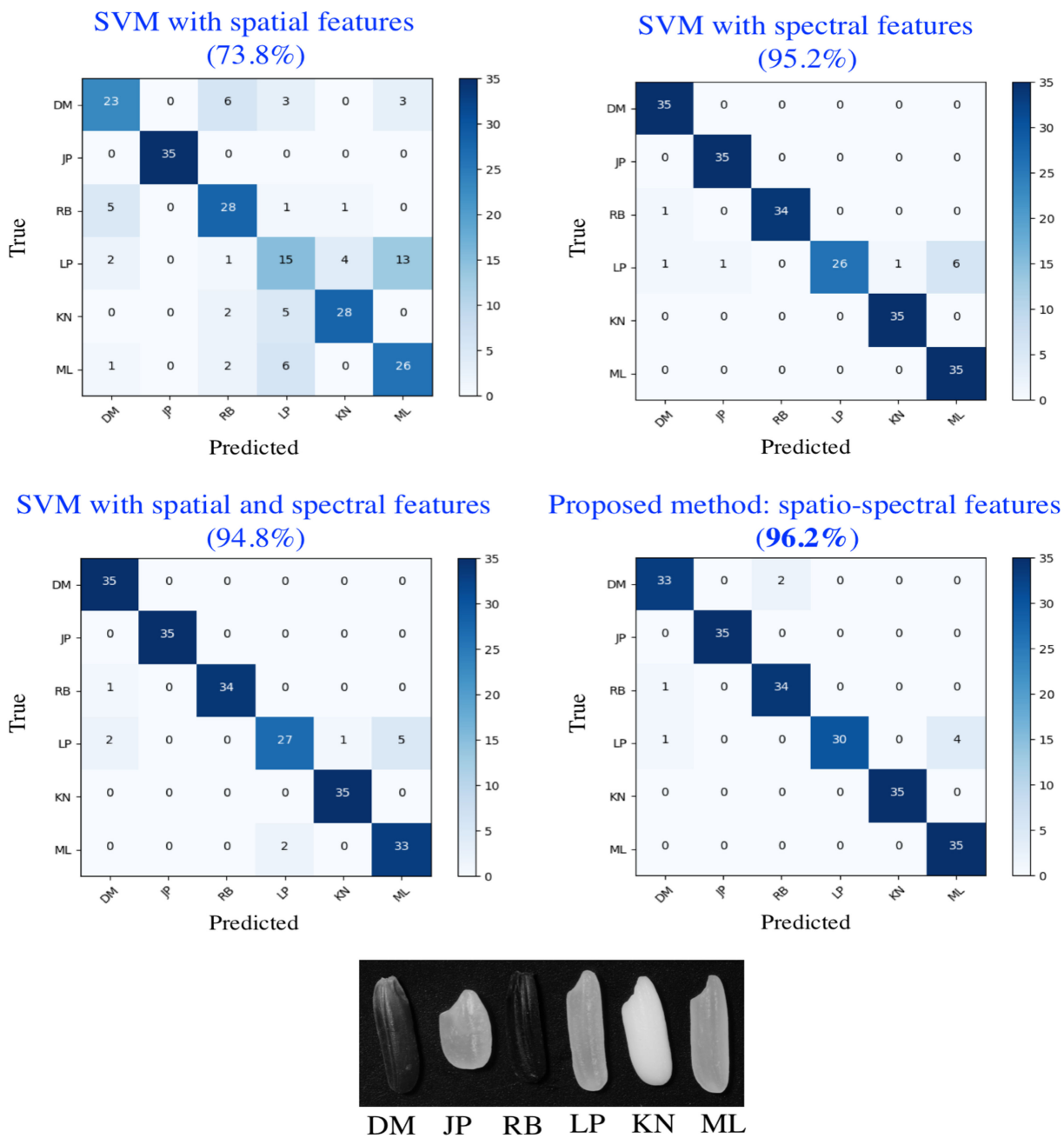


Figure 6. Confusion matrices and classification accuracies of the processed rice dataset. The number in the intersection of the i^{th} row and j^{th} column of each matrix is equal to the number of rice seeds of variety i being misclassified as variety j .

Paddy Rice Dataset: Confusion Matrices and Classification Accuracies

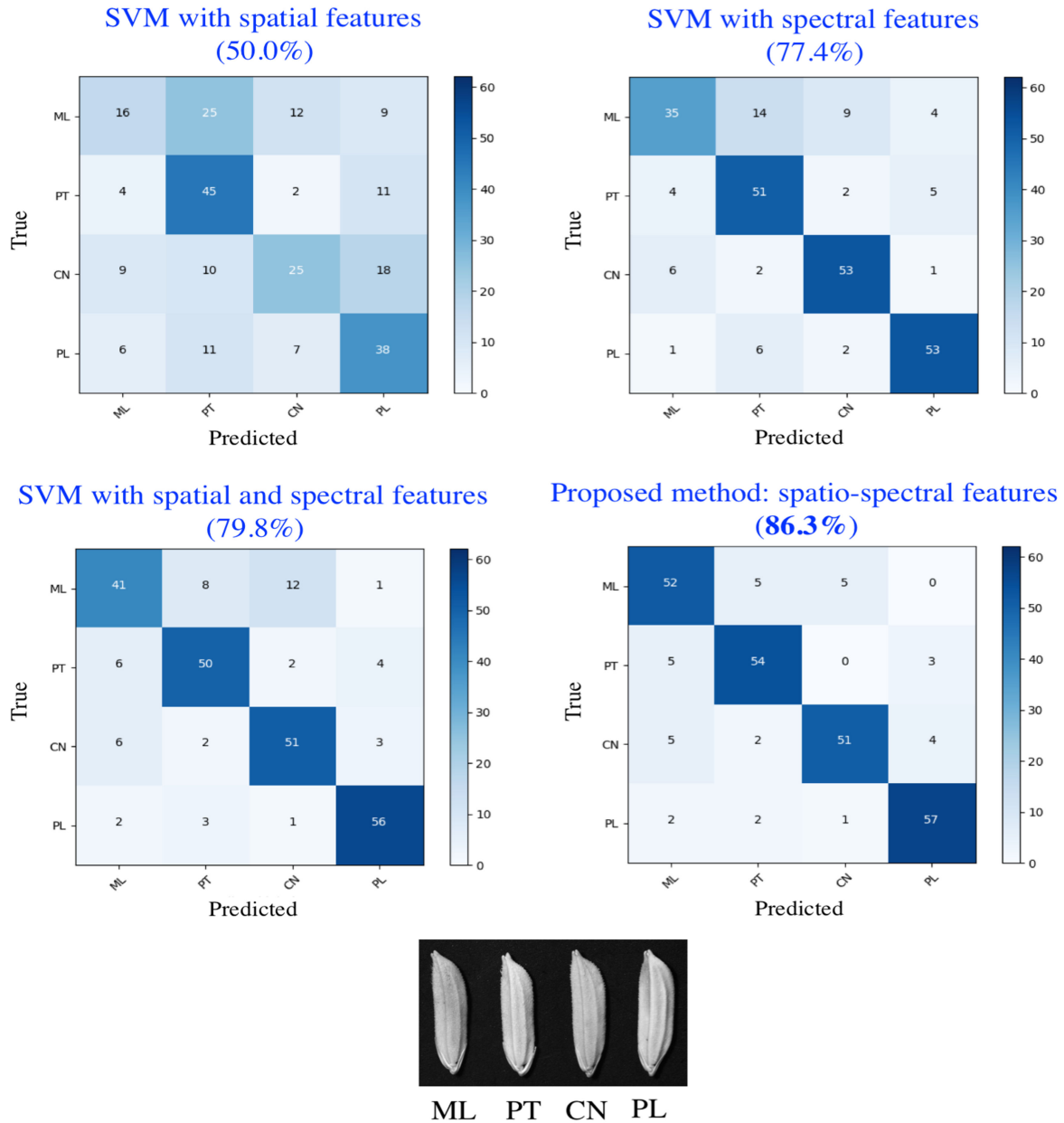


Figure 7. Confusion matrices and classification accuracies of the paddy rice dataset. The number in the intersection of the i^{th} row and j^{th} column of each matrix is equal to the number of rice seeds of variety i being misclassified as variety j .

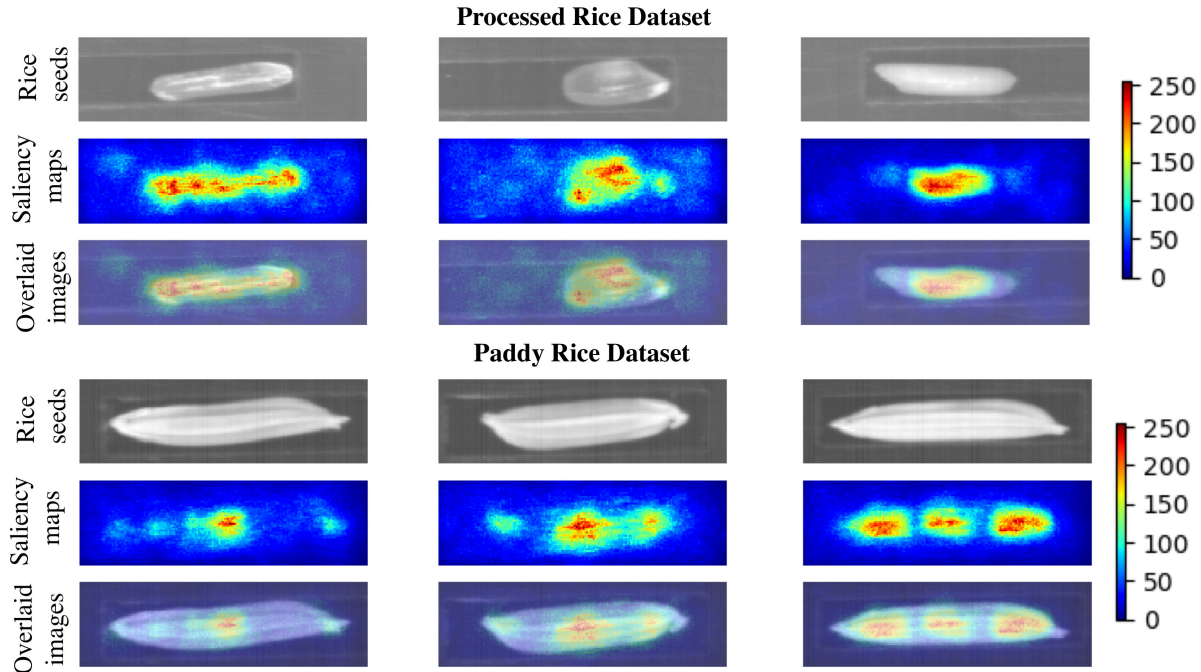


Figure 8. The image-specific saliency maps of some representative rice seeds. The regions with high values in each saliency map contribute more towards the rice variety prediction.

locate the rice seeds in the datacubes and neglect the background regions, bypassing the predefined parameter-dependent rice seed extraction step required in the existing rice variety classification methods [4–15]. Nevertheless, it is not straightforward to tell exactly which specific spatial and/or spectral locations (i.e., voxels) were exploited to distinguish different rice varieties effectively. In general, even with the emerging visualization techniques, it is still challenging to fully make sense of the learned data representations and how the trained network makes a decision, especially for the data with more than two dimensions such as hyperspectral data. Developing new tools to crack open the “black boxes” of deep learning is still an active area of research and should be investigated in future research.

In this work, all the rice seeds were scanned using the hyperspectral imaging system in the same orientation. This fixed-orientation setup simplified the training process of the proposed method. However, for the case when it is more convenient to be able to scan rice seeds in any orientations, it becomes more difficult to train a deep CNN. Specifically, there will be more variations in the datacubes. Consequently, more data will possibly be needed to maintain comparable classification accuracy. In addition to more data acquisition, rotation operations can be included in the data augmentation process to generate more training data.

Although the near-infrared region was selected for this work because of its ability to provide information on chemical properties, which can help distinguish rice varieties, a reasonable extension to the proposed method could be to also acquire information in other regions of the electromagnetic spectrum, and jointly use the complementary information to improve the classification accuracy. Moreover, with the current setup, the proposed system will certainly benefit from higher spatial resolution in terms of classification accuracy, which could be achieved by incorporating a microscope to the data acquisition system along with a speed controller that can reliably maintain the velocity of the conveyor belt, especially when the

velocity becomes very low. In this case, there will be a tradeoff between the classification accuracy and throughput of the inspection system.

In addition to the modifications on the data acquisition part, the data processing and classification part could be improved. Since hyperspectral data can be thought of as a series of images over the spectral axis, Recurrent Neural Networks (RNN) with Long Short Term Memory (LSTM) [56,57] and the Gated Recurrent Unit (GRU) [58] would be potential candidates for improved classification performance because these methods are good at dealing with sequential data.

5. Conclusions

In this work, we proposed a non-destructive rice variety classification method that benefited from the synergy between hyperspectral imaging and spatio-spectral deep learning. Hyperspectral imaging provided not only spatial information, but also spectral information of the rice seeds under inspection. A deep CNN that automatically performed spatio-spectral feature extractions without any predefined data processing steps was used to classify the rice variety of each rice seed. As demonstrated using two types of rice datasets, the proposed method yielded higher classification accuracies than the commonly used classification methods based on SVM. The proposed method achieved 86.3% overall classification accuracy for the paddy rice dataset, which consisted of the rice varieties that have been frequently mistaken for the others, compared to 79.8% obtained from SVM with both spatial and spectral information.

Acknowledgments

We would like to acknowledge the Plant Geoinformatics and Digital Management System Laboratory, National Center for Genetic Engineering and Biotechnology for providing us with the paddy rice seeds.

References

- [1] K.A. Steele, R. Ogden, R. McEwing, H. Briggs, J. Gorham, InDel markers distinguish Basmatis from other fragrant rice varieties, *Field Crops Res.* 105 (2008) 81–87.
- [2] A. Cirillo, S.D. Gaudio, G.D. Bernardo, U. Galderisi, A. Cascino, M. Cipollaro, Molecular characterization of Italian rice cultivars, *Eur. Food Res. Technol.* 228 (2009) 875–881.
- [3] H.Y. Chuang, H.S. Lur, K.K. Hwu, M.C. Chang, Authentication of domestic Taiwan rice varieties based on fingerprinting analysis of microsatellite DNA markers, *Bot. Stud.* 52 (2011) 393–405.
- [4] Z.Y. Liu, F. Cheng, Y.B. Ying, X.Q. Rao, Identification of rice seed varieties using neural network, *J. Zhejiang Univ. Sci. B* 6 (2005) 1095–1100.
- [5] J.D. Guzman, E.K. Peralta, Classification of Philippine rice grains using machine vision and artificial neural networks, *World Conf. Agric. Inf. IT.* (2008) 41–48.
- [6] A.G. OuYang, R.J. Gao, Y.D. Liu, X.D. Sun, Y.Y. Pan, X.L. Dong, An automatic method for identifying different variety of rice seeds using machine vision technology, In *Proc. 2010 Sixth Int. Conf. Nat. Comput.* (2010) 84–88.
- [7] S.J. MousaviRad, F.A. Tab, K. Mollazade, Application of imperialist competitive algorithm for feature selection: a case study on bulk rice classification, *Int. J. Comput. Appl.* 40 (2012) 41–48.

- [8] A.R. Pazoki, F. Farokhi, Z. Pazoki, Classification of rice grain varieties using two artificial neural networks (MLP and neuro-fuzzy), *J. Anim. Plant Sci.* 24 (2014) 336–343.
- [9] P.T.T. Hong, T.T.T. Hai, L.T. Lan, V.T. Hoang, V. Hai, T.T. Nguyen, Comparative study on vision based rice seed varieties identification, In Proc. 2015 Seventh Int. Conf. Knowl. Syst. Eng. (2015) 377–382.
- [10] T.Y. Kuo, C.L. Chung, S.Y. Chen, H.A. Lin, Y.F. Kuo, Identifying rice grains using image analysis and sparse-representation-based classification, *Comput. Electron. Agric.* 127 (2016) 716–725.
- [11] Z.Y. Liu, J.J. Shi, L.W. Zhang, J.F. Huang, Discrimination of rice panicles by hyperspectral reflectance data based on principal component analysis and support vector classification, *J. Zhejiang Univ. Sci. B* 11 (2010) 71–78.
- [12] W. Kong, C. Zhang, F. Liu, P. Nie, Y. He, Rice seed cultivar identification using near-infrared hyperspectral imaging and multivariate data analysis, *Sensors* 13 (2013) 8916–8927.
- [13] L. Wang, D. Liu, H. Pu, D.W. Sun, W. Gao, Z. Xiong, Use of hyperspectral imaging to discriminate the variety and quality of rice, *Food Anal. Methods* 8 (2015) 515–523.
- [14] J. Sun, X. Lu, H. Mao, X. Jin, X. Wu, A method for rapid identification of rice origin by hyperspectral imaging technology, *J. Food Process Eng.* 40 (2017).
- [15] H. Vu, C. Tachtatzis, P. Murray, D. Harle, T.K. Dao, T.L. Le, I. Andonovic, S. Marshall, Spatial and spectral features utilization on a hyperspectral imaging system for rice seed varietal purity inspection, In Proc. 2016 IEEE RIVF Int. Conf. Comput. Commun. Technol. Res. Innov. Vis. Future (2016) 169–174.
- [16] A. Krizhevsky, I. Sutskever, G.E. Hinton, ImageNet classification with deep convolutional neural networks, In Proc. Adv. Neural Inf. Process. Syst. (2012) 1097–1105.
- [17] C. Farabet, C. Couprie, L. Najman, Y. Lecun, Learning hierarchical features for scene labeling, *IEEE Trans. Pattern Anal. Mach. Intell.* 35 (2013) 1915–1929.
- [18] J.J. Tompson, A. Jain, Y. LeCun, C. Bregler, Joint training of a convolutional network and a graphical model for human pose estimation, In Proc. Adv. Neural Inf. Process. Syst. (2012) 1799–1807.
- [19] K. He, X. Zhang, S. Ren, J. Sun, Deep residual learning for image recognition, In Proc. IEEE Conf. Comput. Vis. Pattern Recognit. (2016) 770–778.
- [20] G. Huang, Z. Liu, L. van der Maaten, K.Q. Weinberger, Densely connected convolutional networks, In Proc. IEEE Conf. Comput. Vis. Pattern Recognit. (2017). 4700–4708.
- [21] T. Mikolov, A. Deoras, D. Povey, L. Burget, J. Černocký, Strategies for training large scale neural network language models, In Proc. 2011 IEEE Workshop Autom. Speech Recognit. Underst. (2011) 196–201.
- [22] G. Hinton, L. Deng, D. Yu, G.E. Dahl, A.R. Mohamed, N. Jaitly, V. Vanhoucke, P. Nguyen, T.N. Sainath, B. Kingsbury, Deep neural networks for acoustic modeling in speech recognition, *IEEE Signal Process. Mag.* 29 (2012) 82–97.
- [23] A. Graves, A.R. Mohamed, G. Hinton, Speech recognition with deep recurrent neural networks, In Proc. IEEE Int. Conf. Acoust. Speech Signal Process. (2013) 6645–6649.
- [24] G.E. Dahl, D. Yu, L. Deng, A. Acero, Context-dependent pre-trained deep neural networks for large-vocabulary speech recognition, *IEEE Trans. Audio, Speech Lang. Process.* 20 (2012) 30–42.

- [25] O. Ronneberger, P. Fischer, T. Brox, U-Net: Convolutional networks for biomedical image segmentation, In Proc. Int. Conf. Med. Image Comput. Comput. Interv. (2015) 234–241.
- [26] A. Esteva, B. Kuprel, R.A. Novoa, J. Ko, S.M. Swetter, H.M. Blau, S. Thrun, Dermatologist-level classification of skin cancer with deep neural networks, *Nature* 542 (2017) 115–118.
- [27] R. Poplin, A.V. Varadarajan, K. Blumer, Y. Liu, M.V. McConnell, G.S. Corrado, L. Peng, D.R. Webster, Prediction of cardiovascular risk factors from retinal fundus photographs via deep learning, *Nat. Biomed. Eng.* 2 (2018) 158–164.
- [28] Y. Chen, Z. Lin, X. Zhao, G. Wang, Y. Gu, Deep learning-based classification of hyperspectral data, *IEEE J. Sel. Top. Appl. Earth Obs. Remote Sens.* 7 (2014) 2094–2107.
- [29] W. Hu, Y. Huang, L. Wei, F. Zhang, H. Li, Deep convolutional neural networks for hyperspectral image classification, *J. Sens.* 2015 (2015).
- [30] M.K.K. Leung, H.Y. Xiong, L.J. Lee, B.J. Frey, Deep learning of the tissue-regulated splicing code, *Bioinformatics* 30 (2014) i121–i129.
- [31] H.Y. Xiong, B. Alipanahi, L.J. Lee, H. Bretschneider, D. Merico, R.K.C. Yuen, Y. Hua, S. Gueroussov, H.S. Najafabadi, T.R. Hughes, Q. Morris, Y. Barash, A.R. Krainer, N. Jovic, S.W. Scherer, B.J. Blencowe, B.J. Frey, The human splicing code reveals new insights into the genetic determinants of disease, *Science* 347 (2015) 1254806.
- [32] B.E. Boser, I.M. Guyon, V.N. Vapnik, A training algorithm for optimal margin classifiers, In Proc. Fifth Annu. Workshop. Comput. Learn. Theory (1992) 144–152.
- [33] C. Cortes, V. Vapnik, Support-vector networks, *Mach. Learn.* 20 (1995) 273–297.
- [34] R.M. Haralick, K. Shanmugam, I. Dinstein, Textural features for image classification, *IEEE Trans. Syst. Man Cybern. SMC-3* (1973) 610–621.
- [35] S. van der Walt, J.L. Schönberger, J. Nunez-Iglesias, F. Boulogne, J.D. Warner, N. Yager, E. Gouillart, T. Yu, scikit-image: image processing in Python, *PeerJ.* 2 (2014) e453.
- [36] D.H. Hubel, T.N. Wiesel, Receptive fields, binocular interaction and functional architecture in the cat’s visual cortex, *J. Physiol.* 160 (1962) 106–154.
- [37] Y. Lecun, Y. Bengio, G. Hinton, Deep learning, *Nature* 521 (2015) 436–444.
- [38] I. Goodfellow, Y. Bengio, A. Courville, *Deep Learning*, Cambridge, USA, 2016.
- [39] S. Ioffe, C. Szegedy, Batch normalization: accelerating deep network training by reducing internal covariate shift, In Proc. 32nd Int. Conf. Mach. Learn. 37 (2015) 448–456.
- [40] N. Srivastava, G. Hinton, A. Krizhevsky, I. Sutskever, R. Salakhutdinov, Dropout: a simple way to prevent neural networks from overfitting, *J. Mach. Learn. Res.* 15 (2014) 1929–1958.
- [41] H. Shimodaira, Improving predictive inference under covariate shift by weighting the log-likelihood function, *J. Stat. Plan. Inference* 90 (2000) 227–244.
- [42] G. Bradski, The OpenCV library, *Dr Dobb’s J. Softw. Tools* (2000).
- [43] F. Pedregosa, G. Varoquaux, A. Gramfort, V. Michel, B. Thirion, O. Grisel, M. Blondel, P. Prettenhofer, R. Weiss, V. Dubourg, J. Vanderplas, A. Passos, D. Cournapeau, M. Brucher, M. Perrot, É. Duchesnay, Scikit-learn: machine learning in Python, *J. Mach. Learn. Res.* 12 (2011) 2825–2830.
- [44] F. Chollet and others, Keras, (2015), <https://keras.io>.
- [45] R. Kotikalapudi and contributors, Keras-vis, (2017), GitHub, <https://github.com/raghakot/keras-vis>.

- [46] M. Abadi, P. Barham, J. Chen, Z. Chen, A. Davis, J. Dean, M. Devin, S. Ghemawat, G. Irving, M. Isard, M. Kudlur, J. Levenberg, R. Monga, S. Moore, D.G. Murray, B. Steiner, P. Tucker, V. Vasudevan, P. Warden, M. Wicke, Y. Yu, X. Zheng, TensorFlow: a system for large-scale machine learning (2015).
- [47] D. Kingma, J. Ba, Adam: a method for stochastic optimization, In Proc. Third Int. Conf. Learn. Represent. (2015).
- [48] L.S. Yaeger, R.F. Lyon, B.J. Webb, Effective training of a neural network character classifier for word recognition, In Proc. Adv. Neural Inf. Process. Syst. (1996) 807–813.
- [49] P.Y. Simard, D. Steinkraus, J.C. Platt, Best practices for convolutional neural networks applied to visual document analysis, In Proc. Seventh Int. Conf. Doc. Anal. Recognit. 3 (2003) 958–962.
- [50] D.C. Cireşan, U. Meier, J. Masci, L.M. Gambardella, J. Schmidhuber, High-performance neural networks for visual object classification, arXiv:1102.0183 (2011).
- [51] K. Simonyan, A. Vedaldi, A. Zisserman, Deep inside convolutional networks: visualising image classification models and saliency maps, arXiv:1312.6034 (2013).
- [52] J.T. Springenberg, A. Dosovitskiy, T. Brox, M. Riedmiller, Striving for simplicity: the all convolutional net, In Proc. Third Int. Conf. Learn. Represent. (2015).
- [53] M.D. Zeiler, R. Fergus, Visualizing and understanding convolutional networks, In Proc. Eur. Conf. Comput. Vis. (2014) 818-833.
- [54] J. Yosinski, J. Clune, A. Nguyen, T. Fuchs, H. Lipson, Understanding neural networks through deep visualization, In Proc. 31 St Int. Conf. Mach. Learn. (2015).
- [55] R.R. Selvaraju, M. Cogswell, A. Das, R. Vedantam, D. Parikh, D. Batra, Grad-CAM: visual explanations from deep networks via gradient-based localization, In Proc. IEEE Int. Conf. Comput. Vis. (2017) 618-626.
- [56] S. Hochreiter, J. Schmidhuber, Long short-term memory, Neural Comput. 9 (1997) 1735–1780.
- [57] A. Graves, J. Schmidhuber, Framewise phoneme classification with bidirectional LSTM networks, In Proc. Int. Jt. Conf. Neural Netw. (2005) 2047–2052.
- [58] K. Cho, B. van Merriënboer, C. Gulcehre, D. Bahdanau, F. Bougares, H. Schwenk, Y. Bengio, Learning phrase representations using RNN encoder-decoder for statistical machine translation, In Proc. 2014 Conf. Empir. Methods Nat. Lang. Process. (2014) 1724-1734.